

2-19-2023

A Multicenter Analysis of Nucleic Acid Quantification Using Aqueous Humor Liquid Biopsy in Retinoblastoma: Implications for Clinical Testing

Deborah H Im

Sarah Pike

Mark W Reid

Chen-Ching Peng

Shreya Sirivolu

Follow this and additional works at: <https://jdc.jefferson.edu/willsfp>

See next page for additional authors

 Part of the [Eye Diseases Commons](#), [Neoplasms Commons](#), and the [Ophthalmology Commons](#)

[Let us know how access to this document benefits you](#)

Recommended Citation

Im, Deborah H; Pike, Sarah; Reid, Mark W; Peng, Chen-Ching; Sirivolu, Shreya; Grossniklaus, Hans E; Hubbard, G Baker; Skalet, Alison H; Bellsmith, Kellyn N; Shields, Carol L.; Lally, Sara E; Stacey, Andrew W; Reiser, Bibiana J; Nagiel, Aaron; Shah, Rachana; Xu, Liya; and Berry, Jesse L, "A Multicenter Analysis of Nucleic Acid Quantification Using Aqueous Humor Liquid Biopsy in Retinoblastoma: Implications for Clinical Testing" (2023). *Wills Eye Hospital Papers*. Paper 181.
<https://jdc.jefferson.edu/willsfp/181>

This Article is brought to you for free and open access by the Jefferson Digital Commons. The Jefferson Digital Commons is a service of Thomas Jefferson University's [Center for Teaching and Learning \(CTL\)](#). The Commons is a showcase for Jefferson books and journals, peer-reviewed scholarly publications, unique historical collections from the University archives, and teaching tools. The Jefferson Digital Commons allows researchers and interested readers anywhere in the world to learn about and keep up to date with Jefferson scholarship. This article has been accepted for inclusion in Wills Eye Hospital Papers by an authorized administrator of the Jefferson Digital Commons. For more information, please contact: JeffersonDigitalCommons@jefferson.edu.

Authors

Deborah H Im, Sarah Pike, Mark W Reid, Chen-Ching Peng, Shreya Sirivolu, Hans E Grossniklaus, G Baker Hubbard, Alison H Skalet, Kellyn N Bellsmith, Carol L. Shields, Sara E Lally, Andrew W Stacey, Bibiana J Reiser, Aaron Nagiel, Rachana Shah, Liya Xu, and Jesse L Berry



A Multicenter Analysis of Nucleic Acid Quantification Using Aqueous Humor Liquid Biopsy in Retinoblastoma

Implications for Clinical Testing

Deborah H. Im, BS,^{1,2} Sarah Pike, BA,^{1,2} Mark W. Reid, PhD,¹ Chen-Ching Peng, PhD,^{1,2} Shreya Sivivolu, BA,^{1,2} Hans E. Grossniklaus, MD, MBA,³ G. Baker Hubbard 3rd, MD,³ Alison H. Skalet, MD, PhD,⁴ Kellyn N. Bellsmith, MD,⁴ Carol L. Shields, MD,⁵ Sara E. Lally, MD,⁵ Andrew W. Stacey, MD,⁶ Bibiana J. Reiser, MD,^{1,2} Aaron Nagiel, MD, PhD,^{1,2} Rachana Shah, MD,⁷ Liya Xu, PhD,^{1,2} Jesse L. Berry, MD^{1,2,8,9}

Purpose: Retinoblastoma (RB) is most often diagnosed with clinical features and not diagnosed with tumor biopsy. This study describes tumor-derived analyte concentrations from aqueous humor (AH) liquid biopsy and its use in clinical assays.

Design: Case series study.

Participants: Sixty-two RB eyes from 55 children and 14 control eyes from 12 children from 4 medical centers.

Methods: This study included 128 RB AH samples including: diagnostic (DX) samples, samples from eyes undergoing treatment (TX), samples after completing treatment (END), and during bevacizumab injection for radiation therapy after completing RB treatment (BEV). Fourteen-control AH were analyzed for unprocessed analytes (double-stranded DNA [dsDNA], single-stranded DNA [ssDNA], micro-RNA [miRNA], RNA, and protein) with Qubit fluorescence assays. Double-stranded DNA from 2 RB AH samples underwent low-pass whole-genome sequencing to detect somatic copy number alterations. Logistic regression was used to predict disease burden given analyte concentrations.

Main Outcome Measures: Unprocessed analyte (dsDNA, ssDNA, miRNA, RNA and protein) concentrations.

Results: Results revealed dsDNA, ssDNA, miRNA, and proteins, but not RNA, were quantifiable in most samples (up to 98%) with Qubit fluorescence assays. Median dsDNA concentration was significantly higher in DX (3.08 ng/ μ l) compared to TX (0.18 ng/ μ l; $P < 0.0001$) at an order of 17 times greater and 20 times greater than END samples (0.15 ng/ μ l; $P = 0.001$). Using logistic regression, nucleic acid concentrations were useful in predicting higher versus lower RB disease burden. Retinoblastoma somatic copy number alterations were identified in a TX, but not in a BEV sample, indicating the correlation with RB activity.

Conclusions: Aqueous humor liquid biopsy in RB is a high-yield source of dsDNA, ssDNA, miRNA, and protein. Diagnostic samples are most useful for RB 1 gene mutational analyses. Genomic analysis may be more informative of tumor activity status than quantification alone and can be performed even with smaller analyte concentrations obtained from TX samples.

Financial Disclosure(s): Proprietary or commercial disclosure may be found after the references. *Ophthalmology Science* 2023;3:100289 © 2023 by the American Academy of Ophthalmology. This is an open access article under the CC BY-NC-ND license (<http://creativecommons.org/licenses/by-nc-nd/4.0/>).

Retinoblastoma (RB) is rare among cancers in that it is diagnosed without a tumor biopsy due to concern for seeding tumor outside of the eye.¹ Thus, until recently, there have been no means to identify or quantify tumor-specific biomarkers in RB at diagnosis or during treatment. However, in 2017 we demonstrated that aqueous humor (AH) liquid biopsy is a robust source of tumor derived cell-free DNA (cfDNA) attained via paracentesis.² Aqueous humor liquid biopsy has enabled the identification of multiple tumor-derived analytes.

Our group and others have demonstrated that tumor DNA is present in the AH of eyes with RB and can be utilized to identify retinoblastoma 1 gene (*RBI*) single-nucleotide variants (SNVs), somatic copy number alterations (SCNAs), tumor methylation status, and to estimate tumor fraction.^{2–20} Other groups have evaluated the AH as a liquid biopsy in RB for other analytes including survivin,²¹ metabolomic signatures,¹⁹ expression of secreted peptides,²² and nucleic acids,²³ and in other intraocular tumor types and proteins.²⁴

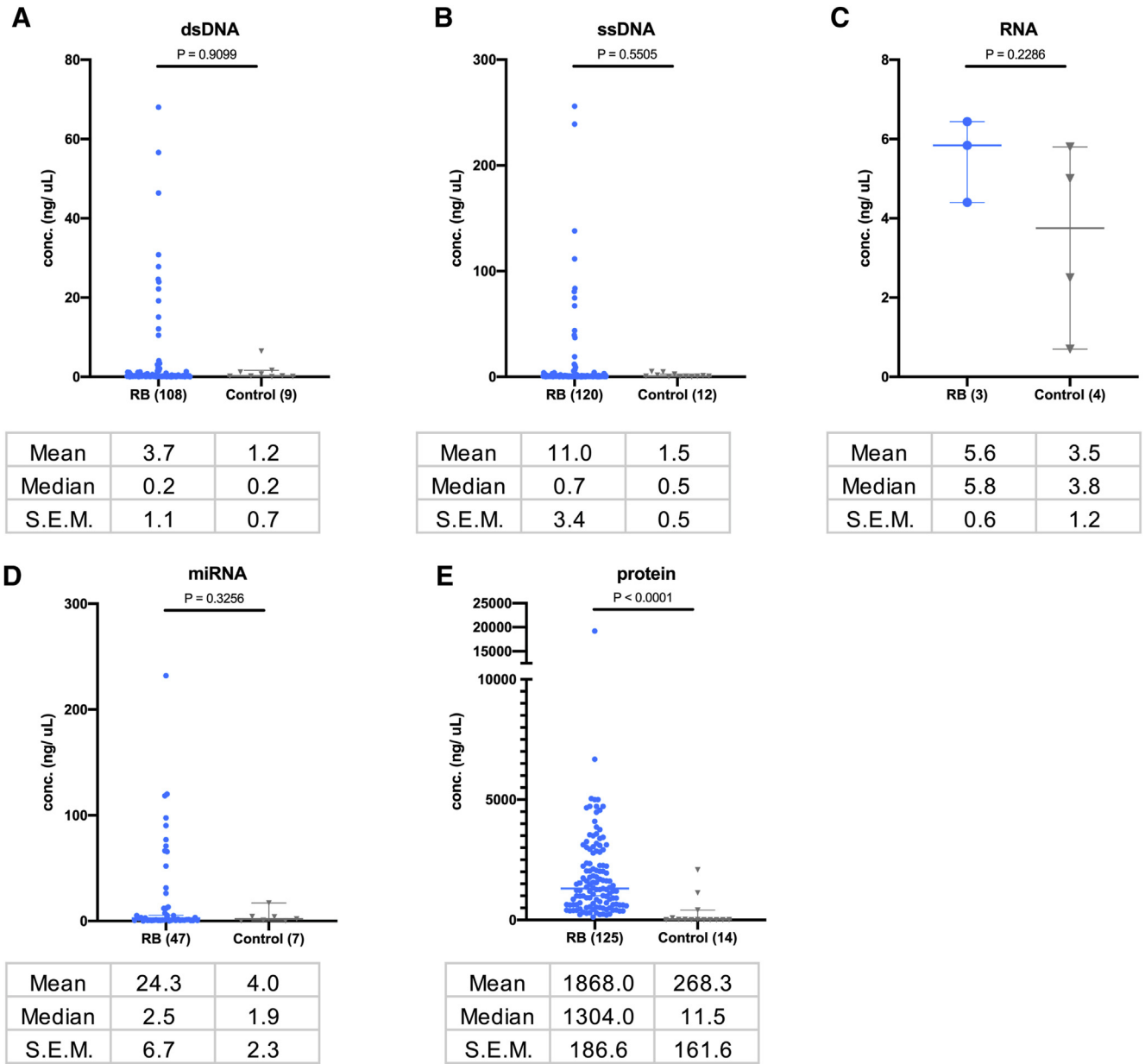


Figure 1. Quantification of aqueous humor analytes in all retinoblastoma (RB) samples and controls: (A) double-stranded DNA (dsDNA), (B) single-stranded DNA (ssDNA), (C) RNA (D) micro-RNA (miRNA), and (E) protein concentration of RB eyes and control eyes were analyzed. SEM = standard error of the mean.

Given the potential clinical application of AH liquid biopsy in RB patients, there is a need for quantification of analytes that may guide the type of genomic analysis testing and biomarker identification that can be done at various clinical time points. Further, quantifying analytes from RB eyes that are treatment-naïve versus actively undergoing treatment may facilitate more accurate and objective ways to determine intraocular disease activity than clinical examination alone.

The purpose of our report is to describe:

(1) The expected concentrations of AH nucleic acids and proteins based on RB International Intraocular

Retinoblastoma Classification (IIRC) Groups and at various therapeutic time points ranging from diagnosis to the end of therapy.

(2) The potential clinical implications for AH liquid biopsy analyses based on quantification of AH analytes and the input needed for various assays.

(3) A stratification of disease burden through logistic modeling based on AH nucleic acids and protein concentration alone.

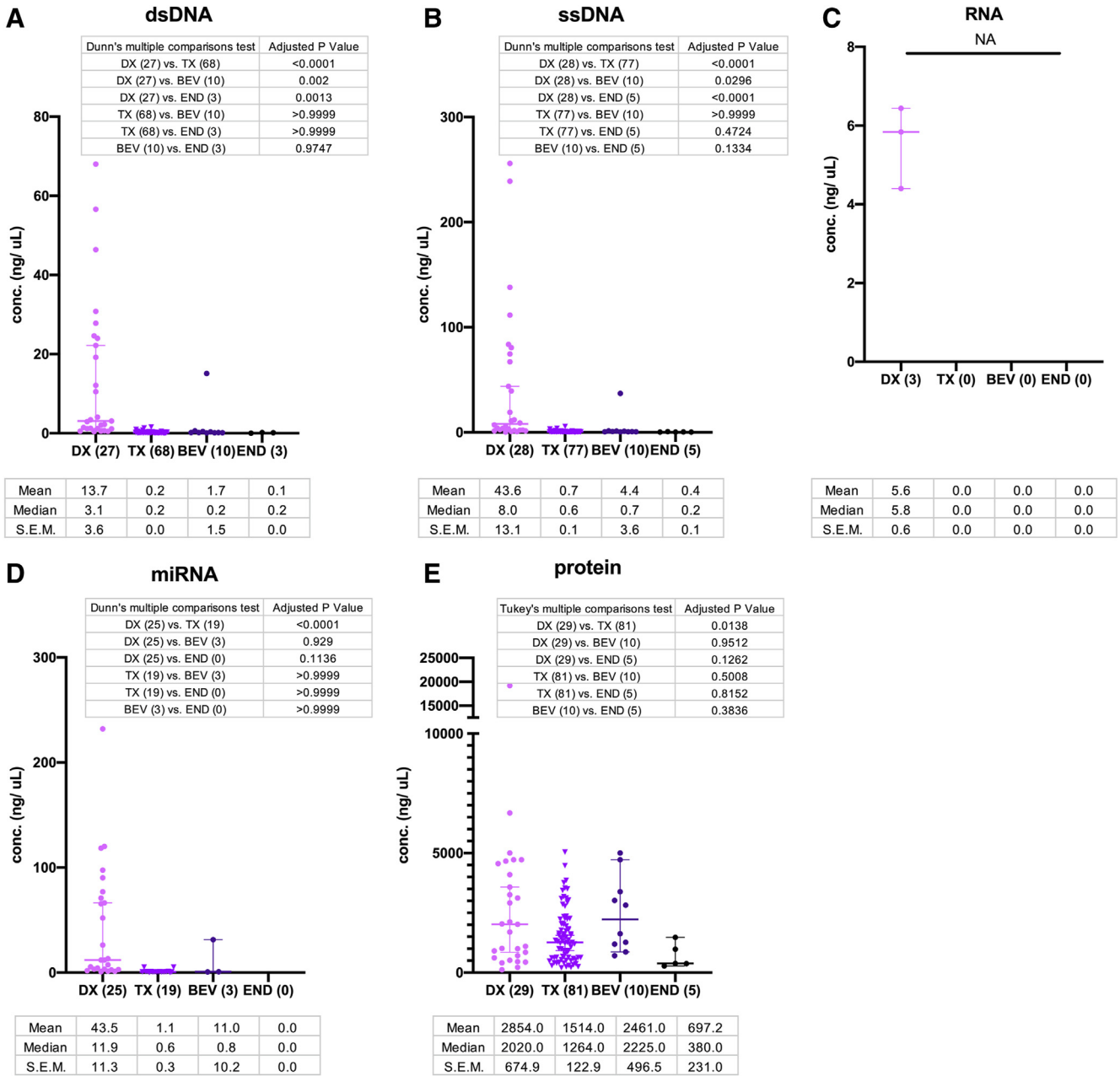


Figure 2. Quantification of retinoblastoma (RB) aqueous humor analytes from: diagnostic (DX), during RB treatment (TX), during bevacizumab injection at the end of RB treatment (BEV), and end of RB treatment (END) samples. **A**, double-stranded DNA (dsDNA), **B** single-stranded DNA (ssDNA), **C** RNA, **D** micro-RNA (miRNA), and **E** protein concentration. NA = not available; SEM = standard error of the mean.

Methods

This investigation is a multicenter case series study at tertiary care hospitals with RB treatment centers. Sites that actively contribute samples to the AH biorepository include: Children’s Hospital Los Angeles, Emory Eye Center, Oregon Health & Science University Hospital Casey Eye Institute, Wills Eye Hospital, and University of Washington Medical Center. All samples were processed in the same laboratory at Children’s Hospital Los Angeles.

Samples were taken between August 2018 and June 2022. Institutional Review Board approval was obtained at each institution for this study. The study was conducted in accordance with the

Declaration of Helsinki. Written informed consent was obtained from the parents of all participants and that included permission for publication.

Specimen Collection and Storage

The detailed methods have been previously published.²⁵ In brief, a paracentesis with extraction of 0.1 ml of AH with a 32-gauge needle was performed. There was no contact between the needle and the retinal tumor or the vitreous cavity. Aqueous humor was extracted at various time points throughout therapy, all while the child was under general anesthesia for routine clinical care for

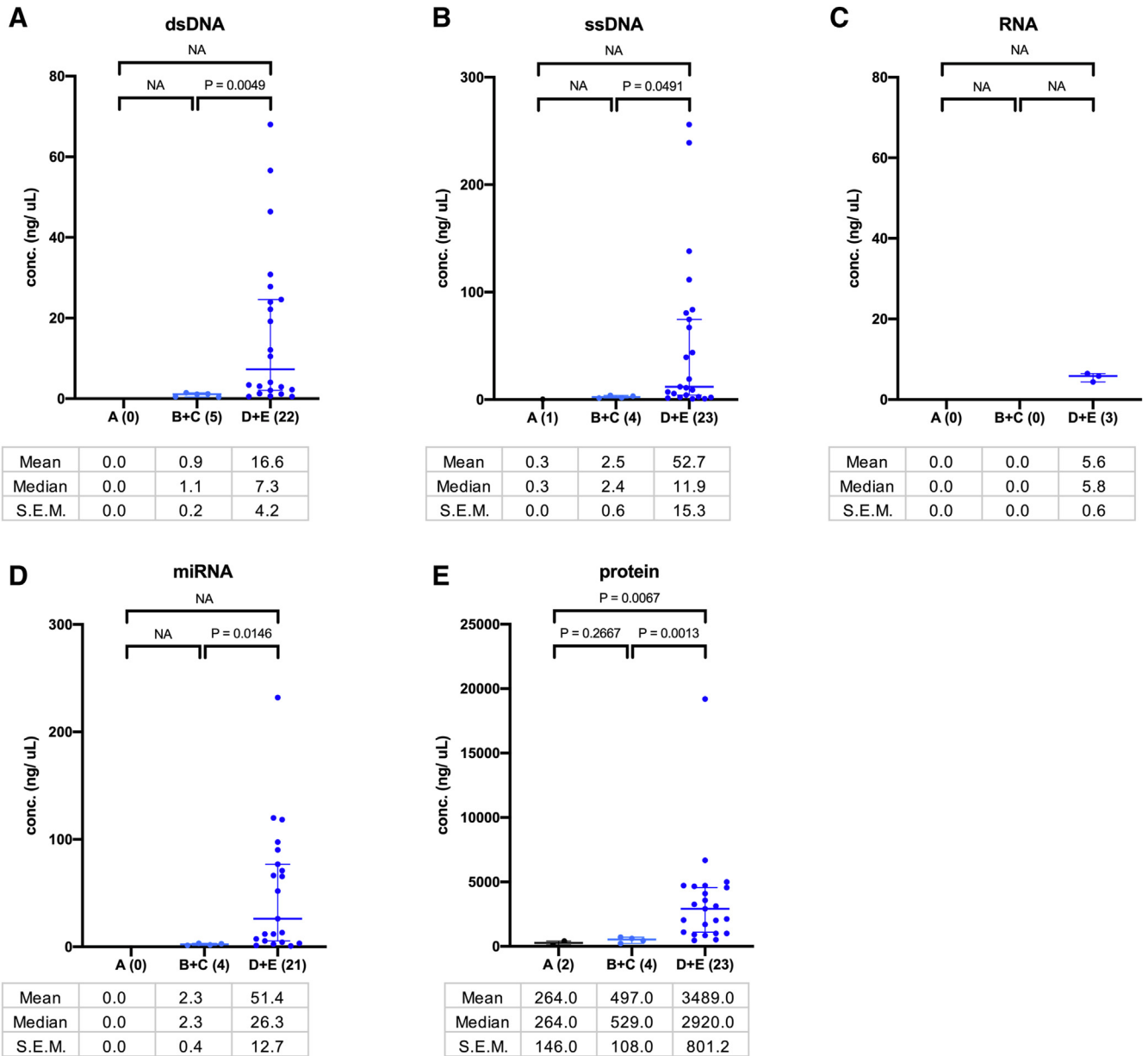


Figure 3. Quantification of retinoblastoma (RB) aqueous humor (AH) analytes from diagnostic AH samples grouped by International Intraocular Retinoblastoma Classification. **A**, double-stranded DNA (dsDNA), **B** single-stranded DNA (ssDNA), **C** RNA, **D** micro-RNA (miRNA), and **E** protein concentration. NA = not available; SEM = standard error of the mean.

their ocular condition. Aqueous humor samples were immediately stored on dry ice and then transferred to a -80°C refrigerator within hours of extraction.

Quantification of Nucleic Acid and Protein Content in AH

Nucleic acids (double-stranded DNA [dsDNA], single-stranded DNA [ssDNA], RNA, and micro-RNA [miRNA]) were assayed using high-sensitivity Qubit Assays for dsDNA and RNA and Qubit Assay Kits for ssDNA and miRNA (Thermo Fisher), with the Qubit Fluorometer following the manufacturer’s manual. Protein concentrations were assayed using the Qubit Protein broad range (BR) assay. The lower limit of detection of these kits are:

- dsDNA = 0.005 ng/ μl
- ssDNA = 0.05 ng/ μl
- RNA = 0.2 ng/ μl
- miRNA = 0.025 ng/ μl
- protein = 100 ng/ μl

Genomic Analysis of Samples

Aqueous humor samples underwent DNA isolation, sequencing, and analysis within 1 month of collection at Children’s Hospital Los Angeles. The methods for this have been previously published.^{4,26} While this was done for each sample the results of genomic sequencing have been (or will be) published separately^{4,5,7–9,27} and are not the focus of this report, aside from an illustrative case study (see Discussion section).

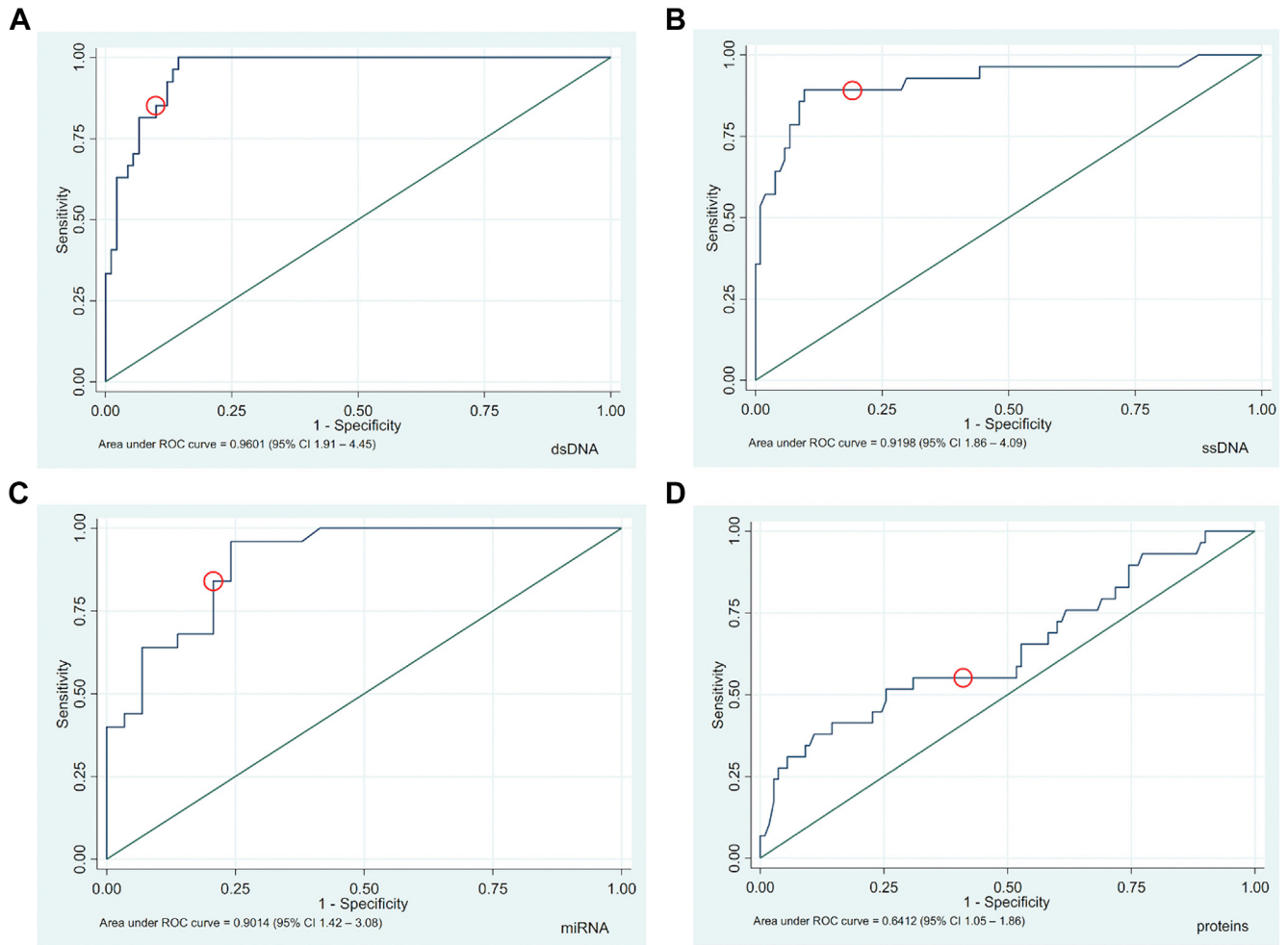


Figure 4. Receiver operating curves (ROC) curve analysis of the utility of aqueous humor analyte concentrations to determine retinoblastoma disease burden. Cut-off values for analyte concentration that maximizes sensitivity and specificity are circled in red. Disease burden was defined as: Highest disease burden (Diagnostic: diagnostic or primarily enucleated samples), Moderate disease burden (During treatment: at secondary enucleation, systemic chemotherapy, intravitreal melphalan injection, or intra-arterial chemotherapy), Lowest disease burden (End of treatment and during bevacizumab injection after the end of treatment). **A**, double-stranded DNA (dsDNA), **B** single-stranded DNA (ssDNA), **C** micro-RNA (miRNA), and **D** protein concentration models. CI = confidence interval.

Statistical Analysis

Analyte concentration samples (dsDNA, ssDNA, miRNA, RNA, and protein) were categorized based on IIRC classification (Groups A–E) of the source eye, as well as disease burden at the time of sample collection. Samples collected at diagnosis prior to subsequent eye-salvage therapy or at primary enucleation were considered diagnostic samples (DX), showing the highest disease burden. Those collected at secondary enucleation, at the time of systemic chemotherapy, intra-arterial chemotherapy, or intravitreal chemotherapy injection were categorized as treatment (TX) samples, reflecting moderate disease burden. Eyes that received bevacizumab injection for radiation retinopathy after completing RB treatment are categorized as sample taken at bevacizumab injection (BEV) and those collected up to 6 months after completing RB treatment were categorized as END samples. Bevacizumab injection and END

samples were from RB patients with no clinical evidence of active intraocular RB tumors or seeding. Samples from eyes diagnosed with conditions other than RB (cataracts, glaucoma, pediatric retinal disease [PRD]) were used as controls.

Differences in analyte values were evaluated overall using Kruskal-Wallis rank tests and tested pairwise using Dunn’s test with Benjamini-Hochberg correction for multiple tests. Analyte concentration values were log-transformed for further evaluation in logistic regression models, which were used to determine cut-off values that distinguish the highest disease burden (DX) from samples with lower burden (TX, BEV, and END) and also examine whether moderate disease burden (TX) could be distinguished from the lowest (BEV and END) based on analyte concentrations. For each analyte, a concentration value was selected that optimized sensitivity and specificity of a given model; these values were back-transformed for use by clinicians. All analyses were conducted using Stata/SE 14.2.

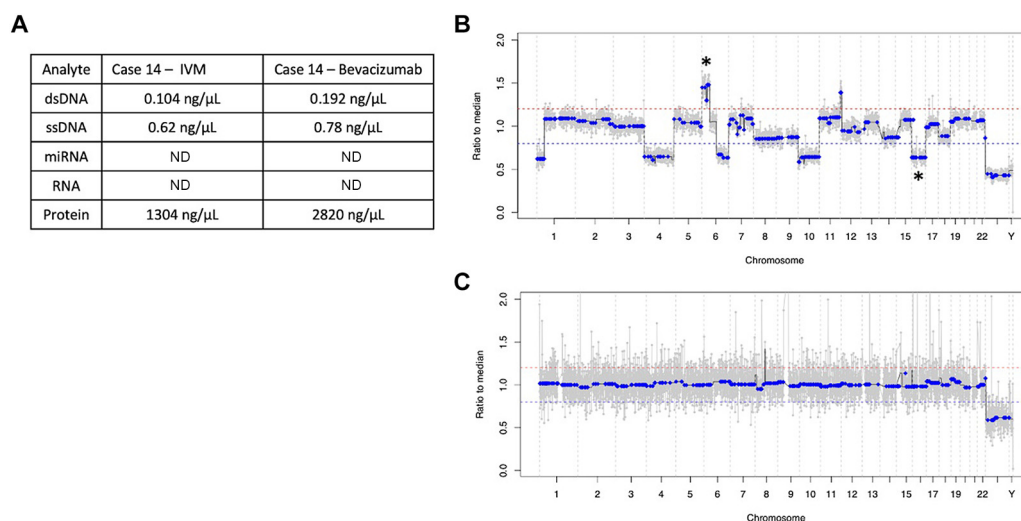


Figure 5. Analyte concentrations and somatic copy number alteration (SCNA) profiles from the same eye at different clinical times. **A**, AH analyte (double-stranded DNA [dsDNA], single-stranded DNA [ssDNA], micro-RNA [miRNA], RNA, and protein) concentrations from Case 14 undergoing intravitreal melphalan (IVM) and the same eye at the end of treatment receiving bevacizumab (BEV) injections. **B**, Case 14 IVM, retinoblastoma SCNAs of 6p gain and 16q loss are indicated with an *. **C**, Case 14 BEV, a flat SCNA profile.

Results

Patient Demographics and AH Sample Characteristics

A total of 128 RB AH samples from 62 RB eyes in 55 children and 14 AH samples from 14 non-RB eyes (3 pediatric cataracts, 2 pediatric glaucoma, and 9 PRD) in 12 children were obtained. No patients had complications secondary to extraction of AH. Thirty-one RB diagnostic AH samples were taken prior to subsequent eye-salvage therapy or at primary enucleation (DX), 82 samples were taken during treatment (TX), 10 samples were taken during bevacizumab injection (BEV), and 5 samples 6 months after completing RB treatment (END). Among DX samples, 2 Group A, 2 Group B, 3 Group C, 20 Group D, and 4 Group E eyes samples were evaluated.

Retinoblastoma tumor IIRC Group, The American Joint Committee on Cancer stage, clinical characteristics, and AH sample characteristics for each case are summarized in [Tables 1](#) and [2](#). The median age for RB patients at diagnosis was 14.5 months (range 11 days–46 months) and median age of control patients was 87.25 months (range 1–208 months).

AH Nucleic Acid (dsDNA, ssDNA, RNA, and miRNA) and Protein Concentrations

All AH samples were stratified by time of sample collection and IIRC classification. Mean (with standard deviation) and median (with range) concentration values for these groupings are shown in [Table 3](#). Most samples demonstrated measurable concentrations of dsDNA (84.4% measurable), ssDNA (95.2%), miRNA (36.7%), and protein (97.7%). Samples that had levels of dsDNA, ssDNA, RNA,

miRNA, and protein below detection thresholds are counted in [Table 3](#) as “ND” (not detected).

Evaluated together, RB AH samples had 113.6 times higher median protein concentrations than Controls, a significant difference (1304 ng/ μ L [118–19 200] vs. 11.48 ng/ μ L [0.30–2080], $P < 0.0001$), but no significant differences were found between RB and control samples for median concentrations of dsDNA, ssDNA, RNA, or miRNA ([Fig 1A–E](#) and [Table 3](#)). It should be noted that AH from eyes with PRD have higher concentrations than cataract or glaucoma samples, but all control AH samples were evaluated collectively due to the limited number available.

Analyte Concentration by Disease Burden

When RB AH samples were further stratified by treatment time point, DX samples had significantly higher analyte concentrations than TX for all analyte types: DX versus TX dsDNA: 3.08 ng/ μ L (0.41–68) versus 0.18 ng/ μ L (0.02–1.57), $P < 0.0001$; ssDNA: 8.03 ng/ μ L (0.28–256) versus 0.56 ng/ μ L (0.10–5.60), $P < 0.0001$; miRNA: 11.90 ng/ μ L (0.80–232) versus 0.64 ng/ μ L (0.06–5.22), $P = 0.009$; protein: 2020 ng/ μ L (118–19 200) versus 1264 ng/ μ L (200–5040), $P = 0.01$; see [Fig 2A–E](#) and [Table 3](#).

DNA concentrations were significantly higher in DX samples compared to BEV and END samples, in which there was no active intraocular disease clinically, for both dsDNA and ssDNA: dsDNA (DX 3.08 ng/ μ L [0.41–68]) versus (BEV 0.19 ng/ μ L [0.11–15.10]; $P = 0.005$) and (END 0.15 ng/ μ L [0.03–0.16]; $P = 0.001$); ssDNA (DX 8.03 ng/ μ L [0.28–256]) versus (BEV 0.72 ng/ μ L [0.38–37]; $P = 0.01$); and (END 0.24 ng/ μ L [0.22–0.68]; $P = 0.04$). Of note, only 3 out of 5 END samples had detectable dsDNA concentrations, but all 5 samples had detectable ssDNA and protein [380 ng/ μ L (276–1474)]. Micro-RNA and RNA concentrations were not detectable in END samples.

Table 1. RB Patient Demographic and Clinical Information

Case ID	Disease	Age at Diagnosis (Months)	Sex	Disease Laterality	Eye Included in Analysis	IIRC at Diagnosis	AJCC	Vitreous Seeding at Diagnosis	Blood RB1 Mutation	Initial Treatment	Required IVM/ IVC?	Required Enucleation?	Time from Diagnosis to Enucleation (Months)	Samples Included in Analysis
1	RB	10	M	U	OS	D	CT2B	None	Negative	IAC	Yes	Yes	22	1
2_OD	RB	2	F	B	OD	E	CT2B	None	c.1421+12_1421+32 del21bp	CEV	Yes	Yes	50	1
2_OS	RB	2	F	B	OS	B	CT1B	None	c.1421+12_1421+32 del21bp	CEV	Yes	No	N/A	1
3	RB	3	F	B	OD	D	CT2B	None	Familial RB, mutation unknown	CEV	Yes	Yes	8	1
4	RB	38	M	B	OD	D	CT2B	Dust and Sphere	c.1961-2A>G	CEV	No	Yes	9	1
5	RB	10	F	U	OS	D	CT3D	Dust	Negative	PE	N/A	Yes	0	1
6	RB	22	M	U	OS	D	CT2B	Sphere	Negative	IAC	Yes	Yes	5	5
7	RB	16	F	B	OS	D	CT2B	None	c.1389+2T>C	PE	N/A	Yes	0	1
8	RB	6	M	U	OD	C	CT1B	Dust	Negative	CEV	Yes	No	N/A	2
9	RB	13	M	B	OS	E	CT3C	Dust	c.1494T>G	CEV	Yes	No	N/A	3
10	RB	4	F	U	OD	D	CT2B	Dust	Negative	CEV	Yes	No	N/A	4
11	RB	18	F	U	OD	D	CT2B	Dust	c.958C>T	CEV	Yes	No	N/A	3
12	RB	19	F	B	OS	D	CT2B	Cloud	c.1875delT	CEV	Yes	No	N/A	5
13	RB	28	M	U	OS	D	CT2B	Dust	c.1847_1848delAA	IAC	Yes	No	N/A	6
14	RB	13	F	U	OS	D	CT2B	Sphere	Negative	IAC	Yes	No	N/A	6
15_OD	RB	4	F	B	OD	B	CT1B	None	c.1666C>T	CEV, IAC	No	No	N/A	2
15_OS	RB	4	F	B	OS	D	CT2B	Dust	c.1666C>T	CEV, IAC	Yes	No	N/A	9
16	RB	8	F	U	OD	D	CT2B	None	Negative	CEV	No	No	N/A	1
17	RB	5	M	U	OS	C	CT2A	None	Negative	CEV	No	No	N/A	2
18	RB	15	F	U	OD	D	CT2B	Sphere and Dust	Negative	CEV	Yes	No	N/A	4
19	RB	18	M	U	OD	D	CT2B	Predominantly cloud	Negative	IAC	No	Yes	1	1
20	RB	35	M	U	OD	D	CT1B	Predominantly cloud	Negative	PE	N/A	Yes	0	1
21	RB	24	F	U	OD	D	CT2B	None	Negative	PE	N/A	Yes	0	1
22	RB	30	M	U	OD	D	CT2B	Dust	Negative	IAC	No	No	N/A	1
23	RB	15	F	U	OS	D	CT2B	Sphere	Negative	PE	N/A	Yes	0	1
24	RB	24	F	U	OD	E	CT3C	Sphere	Negative	PE	N/A	Yes	0	1
25	RB	25	M	U	OD	E	CT3C	Sphere	Negative	PE	N/A	Yes	0	1
26	RB	24	M	U	OS	D	CT2B	Sphere	Negative	IAC	Yes	Yes	5	2
27	RB	18	F	B	OS	D	CT2B	Unknown, presented post treatment	Positive, mutation unknown	CEV	Yes	No	N/A	6
28	RB	24	F	U	OD	E	CT3C	Unknown, filled globe	Negative	PE	N/A	Yes	0	1
29	RB	13	M	U	OS	D	CT2B	Dust	c.607+1G>T	IAC	No	No	N/A	1
30	RB	24	F	U	OD	D	CT2B	Dust	Negative	CEV	Yes	No	N/A	5
31_OD	RB	9	M	B	OD	E	CT2B	Sphere	c.1732delG	CEV	Yes	Yes	19	3
31_OS	RB	9	M	B	OS	D	CT3B	Sphere	c.1732delG	CEV	Yes	Yes	9	2
32_OD	RB	6	M	B	OD	C	CT2B	Dust and Sphere	c.2027T>G	CEV	No	No	N/A	1
32_OS	RB	6	M	B	OS	D	CT2B	Dust	c.2027T>G	CEV	No	No	N/A	1

Im et al • Quantification of RB AH Analytes

(Continued)

Table 1. (Continued.)

Case ID	Disease	Age at Diagnosis (Months)	Sex	Disease Laterality	Eye Included in Analysis	IIRC at Diagnosis	AJCC	Vitreous Seeding at Diagnosis	Blood RB1 Mutation	Initial Treatment	Required IVM/IVC?	Required Enucleation?	Time from Diagnosis to Enucleation (Months)	Samples Included in Analysis
33	RB	19	F	U	OD	D	CT2B	Sphere	Negative	IAC	Yes	Yes	11	5
34	RB	15	F	B	OS	E	CT3C	Unknown, filled globe	Deletion of exons 24–27	CEV	No	Yes	7	1
35	RB	24	M	U	OS	D	CT2B	Filled globe (Cloud, Dust, Sphere)	c.3920T>A	PE	N/A	Yes	0	2
36	RB	24	F	B	OS	D	CT2B	Cloud	c.1362 C>G	IAC	Yes	Yes	9	5
37	RB	24	M	U	OS	D	CT2B	Dust	Negative	CEV	No	Yes	36	2
38	RB	1	F	U	OS	D	CT2B	Dust	Negative	CEV	Yes	No	N/A	4
39	RB	24	F	U	OD	D	CT2B	Cloud	Negative	PE	N/A	Yes	0	1
40_OD	RB	2	M	B	OD	A	CT1A	None	c.607+1G>C	Laser	No	No	N/A	1
40_OS	RB	2	M	B	OS	A	CT1A	None	c.607+1G>C	Laser	No	No	N/A	1
41	RB	8	F	U	OD	D	CT2B	Sphere	c.1362C>G	CEV	Yes	No	N/A	2
42_OD	RB	27	F	B	OD	A	CT1A	None	c.1399C>T	Laser	No	No	N/A	1
42_OS	RB	27	F	B	OS	D	CT2B	Cloud	c.1399C>T	CEV	No	Yes	7	1
43	RB	35	M	U	OS	D	CT2B	Cloud	Negative	CEV	Yes	No	N/A	1
44_OD	RB	4	F	B	OD	B	CT1B	None	c.1215+1G>A	CEV, Laser	No	No	N/A	1
44_OS	RB	4	F	B	OS	C	CT2B	None	c.1215+1G>A	CEV	No	No	N/A	1
45	RB	46	M	U	OS	D	CT2B	None	Negative	CEV	No	No	N/A	1
46	RB	4	M	U	OS	C	CT2B	None	c.958C>T	CEV	No	No	N/A	1
47	RB	8	F	U	OS	D	CT2B	Sphere	Negative	CEV	No	No	N/A	1
48	RB	6	M	U	OD	D	CT2B	Unknown, filled globe	Negative	CEV	No	No	N/A	1
49	RB	20	F	U	OD	D	CT2B	Cloud	Positive, mutation unknown	IAC	Yes	No	N/A	1
50	RB	36	M	B	OS	E	CT2B	Cloud	Positive, mutation unknown	IAC	Yes	No	N/A	1
51	RB	< 1 (11 days)	F	B	OD	A	CT1A	None	N/A	CEV	Yes	No	N/A	1
52	RB	10	M	U	OD	D	CT2B	Cloud	Negative	IAC	Yes	No	N/A	1
53	RB	4	F	U	OD	E	CT3C	None	Negative	PE	N/A	Yes	0	1
54	RB	14	F	U	OS	C	CT1B	None	Positive, mutation unknown	IAC	Yes	Yes	Unknown	1
55	RB	22	F	U	OS	D	CT2B	Sphere	Negative	IAC	Yes	Yes	Unknown	1

AJCC = American Joint Committee on Cancer; B = bilateral disease; CEV = systemic carboplatin [C]/etoposide[E]/vincristine[V]; F = female; IAC = intra-arterial chemotherapy; Case ID = case identification; IIRC = International Intraocular Retinoblastoma Classification; IVC = intravenous chemotherapy; IVM = intravitreal melphalan; M = male; N/A = not applicable; OD = right eye; OS = left eye; PE = primary enucleation; RB = retinoblastoma; RB1 = retinoblastoma 1 gene; U = unilateral disease.

Table 2. Control Sample Demographic Information

Case ID	Diagnosis	Age at Diagnosis (Months)	Sex	Disease Laterality	AH Sample Eye
Ret09	PRD	92	M	U	OD
Ret011	PRD	181.9	F	U	OD
Ret017	PRD	36	M	U	OS
Ret018	PRD	181.7	M	U	OS
Ret013	PRD	146	M	U	OD
Ret014	PRD	204	M	B	OD
Ret014	PRD	204	M	B	OS
Ret019	PRD	208	M	U	OD
Ret015	PRD	82.5	M	U	OS
Glc05	Pediatric Glaucoma	4	M	B	OD
Glc09	Pediatric Glaucoma	50	F	U	OD
Cat07	Pediatric Cataract	55	M	B	OD
Cat07	Pediatric Cataract	55	M	B	OS
Cat08	Pediatric Cataract	1	M	U	OD

AH = aqueous humor; B = bilateral disease; F = female; Case ID = case identification; M = male; OD = right eye; OS = left eye; PRD = pediatric retinal disease; U = unilateral disease.

Analyte Concentrations at Diagnosis by IIRC Group

Diagnostic samples were evaluated by IIRC Groups and are shown in Table 3. Out of only 2 Group A DX samples, proteins were detectable in both (264 ng/μl [118–410]), but only 1 sample yielded detectable ssDNA concentration (0.28 ng/μl) and other nucleic acids were undetectable. Samples from eyes with moderate disease (Groups B and C) were compared to those with more extensive disease (Groups D and E). As shown in Figure 3A–E, analyte concentrations in Group D/E eyes were significantly higher than concentrations in Group B/C eyes: dsDNA: 7.29 ng/μl (2.10–24.60) versus 1.11 ng/μl (0.47–1.18), $P = 0.005$; ssDNA: 11.90 ng/μl (2.60–80.60) versus 2.41 ng/μl (1.55–3.5), $P = 0.049$; miRNA: 26.30 ng/μl (5.48–77) versus 2.32 ng/μl (1.61–3), $P = 0.01$; protein: 2920 ng/μl (1008–4660) versus 529 ng/μl (330–664), $P = 0.001$; see Figure 3A–E.

Analyte Concentrations as Predictors of RB Disease Burden

Analyte concentrations were used to predict RB disease burden (e.g., DX vs. TX vs. END) in logistic regression models. As illustrated in Figure 4A–D, sample concentrations were useful predictors of whether a sample was obtained from an eye with the highest disease burden. Aqueous humor concentration cut-offs of dsDNA 0.61 ng/μl (89% accuracy), ssDNA 1.38 ng/μl (90% accuracy) and miRNA 2.4 ng/μl (81% accuracy) were able to distinguish higher and lower disease burden, with higher analyte concentrations correlating to higher disease burden. Protein concentrations were less useful in identifying highest disease burden, where concentration of 1310 ng/μl could be used to identify a sample with highest disease burden eye with only 56% accuracy. Logistic model calculations were not performed on RNA concentrations due to insufficient quantifiable RNA samples. Analyte concentrations were not

useful in distinguishing moderate disease burden (TX) from low-disease burden samples (END or BEV).

Clinical Correlates of RB Somatic Copy Number Alteration Analysis

As previously reported, common highly recurrent RB SCNAs include 1q, 2p and 6p gain, and 16q and 13q loss are identifiable in AH samples.^{4,7,8,28} To demonstrate the impact of SCNA analysis versus analyte quantification alone, 2 representative AH samples from the same eye at 2 different clinical time points involving intravitreal injections were examined; one obtained during RB therapy using intravitreal chemotherapy for treating seeds and 1 at the end of therapy during bevacizumab injection to treat radiation retinopathy (Fig 5A). Both TX and BEV samples had similar dsDNA, ssDNA, and protein analyte concentrations, while miRNA and RNA levels were undetectable. The SCNA profile of a sample taken during intravitreal chemotherapy displayed RB SCNAs of 6p gain, as well as 16q loss (Fig 5B). The genomic profile of an RB case undergoing additional bevacizumab injections had no discernable SCNAs on whole genome sequencing (Fig 5C).

Discussion

This is a multicenter study analyzing the use of AH liquid biopsy with 128 RB AH and 14 Control AH samples to investigate the quantification of AH nucleic acid and protein analytes. Herein we demonstrate that (1) the AH is a high-yield source of multiple circulating analytes (dsDNA, ssDNA, miRNA, and protein) in RB with concentrations that can be measured at diagnosis and through therapy, (2) AH analyte (dsDNA, ssDNA, miRNA, and protein) concentrations were highest in samples taken before treatment (DX), either at diagnosis or primary enucleation, and (3) analyte concentrations alone during treatment may not be sufficient in determining whether or not there is active

Table 3. Sample Analyte Ranges Including Mean, Median, and Number of AH Samples for dsDNA, ssDNA, RNA, miRNA, and Protein by Time of AH Sample, Disease Type, and Burden

Diagnosis	dsDNA (ng/μl)				ssDNA (ng/μl)				RNA (ng/μl)				miRNA (ng/μl)				Protein (ng/μl)			
	Sample Size		Mean ± SD	Median (Range)	Sample Size		Mean ± SD	Median (Range)	Sample Size		Mean ± SD	Median (Range)	Sample Size		Mean ± SD	Median (Range)	Sample Size		Mean ± SD	Median (Range)
	#Read	ND			#Read	ND			#Read	ND			#Read	ND			#Read	ND		
RB AH taken at Diagnosis* (n = 31)	27	4	13.65 ± 18.63	3.08 (0.41–68)	28	1	43.62 ± 69.06	8.03 (0.28–256)	3	22	5.56 ± 1.05	5.84 (4.40–6.44)	25	4	43.51 ± 56.37	11.9 (0.80–232)	29	0	2853 ± 3635	2020 (118–19200)
All Samples (n = 128)	108	20	3.74 ± 10.93	0.22 (0.02–68)	120	6	11.04 ± 37.67	0.68 (0.10–256)	3	117	5.56 ± 1.05	5.84 (4.40–6.44)	47	79	24.3 ± 45.89	2.5 (0.06–232)	125	1	1868 ± 2086	1304 (118–19200)
By Eye Classification AH taken at Diagnosis*:																				
A (n = 2)	0	2	—	—	1	1	0.28	0.28	0	2	—	—	0	2	—	—	2	0	264 ± 206	264 (118–410)
B (n = 2)	2	0	1.15 ± 0.05	1.18 (1.11–1.18)	1	0	3.12	3.12	0	1	—	—	1	0	2.78	2.78	1	0	220	220
C (n = 3)	3	0	0.78 ± 0.59	0.47 (0.41–1.46)	3	0	2.32 ± 1.36	1.7 (1.39–3.88)	0	3	—	—	3	0	2.14 ± 0.97	1.86 (1.35–3.22)	3	0	589 ± 137	618 (440–710)
D (n = 20)	18	2	14.9 ± 16.86	7.29 (0.51–56.6)	19	0	43.87 ± 61.19	11.9 (0.64–239)	1	14	6.44	6.44	17	2	42.25 ± 39.78	26.3 (0.80–120)	19	0	2527 ± 1785	2040 (460–6680)
E (n = 4)	4	0	23.99 ± 31.27	13.35 (1.27–68)	4	0	94.34 ± 118.94	58.6 (4.14–256)	2	2	5.12 ± 1.02	5.12 (4.4–5.84)	4	0	90.06 ± 108.71	61.94 (4.34–232)	4	0	8055 ± 7449	4720 (3580–19200)
Diagnosis	dsDNA (ng/μl)				ssDNA (ng/μl)				RNA (ng/μl)				miRNA (ng/μl)				Protein (ng/μl)			
	Sample Size		Mean ± SD	Median (Range)	Sample Size		Mean ± SD	Median (Range)	Sample Size		Mean ± SD	Median (Range)	Sample Size		Mean ± SD	Median (Range)	Sample Size		Mean ± SD	Median (Range)
	#Read	ND			#Read	ND			#Read	ND			#Read	ND			#Read	ND		
By Disease Burden																				
Highest* (n = 31)	27	4	13.65 ± 18.63	3.08 (0.41–68)	28	1	43.62 ± 69.06	8.03 (0.28–256)	3	22	5.56 ± 1.05	5.84 (4.40–6.44)	25	4	43.51 ± 56.37	11.9 (0.80–232)	29	0	2853 ± 3635	2020 (118–19200)
Moderate** (n = 82)	68	14	0.25 ± 0.26	0.18 (0.02–1.57)	77	5	0.75 ± 0.79	0.56 (0.10–5.6)	0	81	—	—	19	63	1.12 ± 1.46	0.64 (0.06–5.22)	81	1	1514 ± 1106	1264 (200–5040)
Bevacizumab at the End of RB Treatment*** (n = 10)	10	0	1.74 ± 4.7	0.193 (0.114–15.1)	10	0	4.42 ± 11.5	0.72 (0.38–37)	0	10	—	—	3	7	11 ± 17.7	0.8 (0.68–31.4)	10	0	2461 ± 1570	2225 (710–5000)
End of RB Treatment**** (n = 5)	3	2	0.114 ± 0.075	0.152 (0.028–0.162)	5	0	0.352 ± 0.198	0.24 (0.22–0.68)	0	5	—	—	0	5	—	—	5	0	697 ± 516	380 (276–1474)
Other Conditions																				
Cataracts	9	5	1.2 ± 2.06	0.23 (0.07–6.50)	12	2	1.46 ± 1.73	0.54 (0.11–4.98)	4	10	3.5 ± 2.34	3.75 (0.7–5.8)	7	7	3.99 ± 5.97	1.91 (0.16–17)	14	0	268 ± 605	11.48 (0.30–2080)
Glaucoma	0	3	—	—	1	2	0.24	0.24	0	3	—	—	0	3	—	—	3	0	169 ± 208	80 (20–406)
PRD	2	0	0.09 ± 0.03	0.09 (0.07–0.11)	2	0	0.51 ± 0.01	0.51 (0.50–0.52)	0	2	—	—	0	2	—	—	2	0	1602 ± 676	1602 (1124–2080)
	7	2	1.52 ± 2.27	0.74 (0.13–6.50)	9	0	1.8 ± 1.89	1.03 (0.11–4.98)	4	5	3.5 ± 2.34	3.75 (0.7–5.8)	7	2	3.99 ± 5.97	1.91 (0.16–17)	9	0	5.18 ± 5.99	1.75 (0.30–14.96)

AH = aqueous humor; dsDNA = double-stranded DNA; miRNA = micro-RNA; ND = not detected; PRD = pediatric retinal disease; RB = retinoblastoma; SD = standard deviation; ssDNA = single-stranded DNA.
Highest disease burden: *Includes samples taken at diagnosis prior to any subsequent treatment and at primary enucleation. Moderate disease burden: **During treatment, during intravitreal melphalan, intra-arterial chemotherapy, systemic chemotherapy or at secondary enucleation. Lowest disease burden: ***End of RB treatment during bevacizumab injection and ****End of RB treatment.
#Read indicates the number of samples with detectable levels of each analyte. ND, not detected, indicates the number of samples with a concentration too low for detection.

intraocular disease, but the addition of genomic analysis may be more useful. To the authors' knowledge, this is the first multicenter report that investigates quantifiable analytes in AH liquid biopsy of RB and has important implications for future use of the AH in clinical assays of various analytes as a diagnostic and prognostic liquid biopsy.

Herein we report mean and median nucleic acid (dsDNA, ssDNA, miRNA) and protein concentrations from diagnosis to the end of treatment (Table 3). Most analytes were readily detectable from diagnosis through therapy. However, RNA was only detectable in DX samples with Qubit high sensitivity RNA assay, likely due to high degree of degradation. This RNA assay is designed to detect RNA fragments longer than 100 nucleotides. Aqueous humor RNA may be better detected using other methods. For dsDNA, median concentrations from DX AH samples were on the order of 17 times higher than TX, 16 times higher than BEV, and 20 times higher than END samples. Diagnostic AH sample concentrations were also significantly higher than TX samples for dsDNA, ssDNA, miRNA, and protein (Fig 2A–E). Diagnostic samples had higher concentrations than BEV (Fig 2A) and END (Fig 2B) samples for dsDNA and ssDNA. As hypothesized, DX concentrations had the highest concentration of all analytes, which implicates DX AH liquid biopsy as a promising liquid biopsy source of tumor-derived analytes for various RB research and clinical assays.

International Intraocular Retinoblastoma Classification Groups also correlated with analyte concentrations, with more severe Groups D and E having higher analyte concentrations. When comparing DX samples from different IIRC Groups, Groups E dsDNA median concentrations were on the order of 1.8 times higher than Group D, 28.4 times greater than Group C, and 11.3 times greater than Group B; almost directly correlating to the increase in tumor size between Groups. Group A samples had mostly undetectable nucleic acid concentrations. Group D and E eyes had significantly higher concentrations than Group B and C for dsDNA, ssDNA, miRNA, and protein, but not RNA (Fig 3A–E). This demonstrates that DX AH samples from all except Group A eyes with the smallest tumor (< 3 mm tumors) are expected to have detectible analyte concentrations.

We then investigated AH analyte concentrations' relationship to disease burden, defined by DX and primary enucleation samples as highest disease burden. With a logistic regression model using analyte concentrations, we found dsDNA, ssDNA, and miRNA levels were useful in predicting disease burden, with higher values clearly defining greater disease burden. All nucleic acid (dsDNA, ssDNA, and miRNA) models were strongly correlated with one another, while protein levels were less useful in distinguishing disease burden (Fig 4A–D). Diagnostic samples could be identified by AH concentration cut-offs of dsDNA 0.61 ng/μl, ssDNA 1.38 ng/μl, and miRNA 2.4 ng/μl with 81% to 90% accuracy, where concentrations greater than these cut-offs correlated with higher disease burden. Thus, at diagnosis, in the setting of a diagnostic dilemma, analyte concentration alone may be useful, along with facilitating specific genetic and genomic assays. However, eyes that were undergoing therapy and eyes at the end of RB therapy

were not distinguishable with nucleic acid concentrations alone in this sample.

What are the implications of this data? Our group and others have already demonstrated that the AH cfDNA can be utilized to identify *RBI* SNVs, SCNAs, tumor methylation status, and to estimate tumor fraction.^{2–20} However, as the AH liquid biopsy moves from an area of bench research to one of standard-of-care clinical assays, the expected ranges of analytes at different clinical time points will impact the kind of analyses that can be done. For example, next-generation sequencing for SNV analysis of genetic mutations requires target enrichment and a higher DNA input in any sample (whether AH or another liquid biopsy source). Thus, only treatment naive AH samples, with a median 3.08 ng/μl, may routinely provide enough DNA for next-generation sequencing *RBI* gene mutation analysis. Le Gall et al¹⁶ also reported that AH DNA concentration was too low to perform gene analysis in a patient after several intravitreal melphalan treatments. While this technology continues to improve, the current clinical industry standard for SNV analysis requires > 20 ng of dsDNA input⁶ which can be found in as little as 10 μl from a DX sample or require > 100 μl during therapy. However, current laboratory developed tests for research require lower concentrations, demonstrating that reliable results are possible with lower inputs. During treatment, the concentration of DNA in the AH may or may not be adequate for *RBI* mutation analysis, but at diagnosis, it is adequate in nearly all cases.

However, that is not to say there is no utility of AH analysis at other clinical time points. While a lower concentration of AH cfDNA is found in samples taken during RB treatment (e.g., dsDNA, with a median concentration of 0.18 ng/μl), this amount is sufficient to perform genomic analysis via low-pass whole-genome sequencing,¹⁵ as seen in Figure 5B. The advantage of SCNA identification is multifold. First, SCNA analysis requires a lower DNA concentration than SNV analysis, so it can be done even when the tumor burden is low²⁵. Furthermore, SCNAs can also be utilized to determine tumor fraction, which correlates to intraocular disease activity.²⁹

Aside from establishing expected concentrations of analytes at various clinical time points, we also wanted to evaluate whether evaluation of AH concentration alone could help indicate that a tumor is active. While ocular oncologists currently do this based on clinical examination, this is significantly hampered if there is a loss of view to the back of the eye. This can happen due to various reasons including vitreous hemorrhage, and anti-VEGF agents are often given intravitreally³⁰. Although BEV AH samples were thought to not have clinically active RB, we predicted that the presence of vitreous hemorrhage secondary to radiation retinopathy would affect analyte concentrations. As hypothesized, TX and BEV AH samples had similar analyte concentrations (dsDNA: TX, 0.104 ng/μl; BEV 0.192 ng/μl), but these values are not significantly different from the median dsDNA concentration observed in AH samples from patients with PRD (0.74 ng/μl; see Table 3). Thus, in the setting of loss of view due to vitreous hemorrhage, AH analyte concentrations alone cannot indicate whether the

RB tumor is active in the eye, except for a large tumor at diagnosis. However, genomic analysis of the AH may provide additional objective evidence of the resolution of the RB tumor. For example, in the same eye at different clinical time points and with similar analyte concentrations between the samples, there were no SCNAs identified in the BEV AH, while the TX AH had positive RB SCNAs 6p gain, and 16q loss^{4,7,8,28} (Fig 5A–C). We suggest that the positive RB SCNAs reflect the presence of active RB tumor, as we expected in an eye undergoing treatment (Fig 5B). Thus, identification of SCNA via low-pass whole-genome sequencing analysis may provide additional disease status information beyond analyte concentration, especially in the presence of vitreous hemorrhage.

A limitation in this report is our small sample size from each disease burden group, since a larger cohort would produce a better powered model. Further investigations with larger sample sizes from multiple centers should be pursued for further validation of our results.

In summary, AH liquid biopsy at the time of diagnosis, prior to any therapy, provides the highest nucleic acid and

protein concentrations, and may be most useful for *RBI* mutational testing. Aqueous humor biopsy during therapy can also yield high enough dsDNA concentration to perform low-pass whole-genome sequencing and SCNA detection to facilitate prognosis and trends in tumor fraction which correlate with ocular outcomes.^{7–9} Nucleic acid quantifications can stratify high- versus low-disease burden eyes and higher analyte concentrations correlated with increasing IIRC group and disease burden; however, it was not possible to reliably distinguish low-disease burden from eyes without active disease (TX vs. BEV/END), which may be complicated by vitreous hemorrhage. Aqueous humor liquid biopsy is a high-yield source of nucleic acids and proteins in RB specifically at diagnosis. Evaluating AH analyte quantifications will facilitate potential applications of clinical assays.

Acknowledgments

The authors would like to acknowledge Brianne Brown for the coordination of this study.

Footnotes and Disclosures

Originally received: December 13, 2022.

Final revision: February 7, 2023.

Accepted: February 13, 2023.

Available online: February 19, 2023. Manuscript no. XOPS-D-22-00267.

¹ Department of Surgery, Division of Ophthalmology, The Vision Center at Children's Hospital Los Angeles, Los Angeles, California.

² USC Roski Eye Institute, Keck School of Medicine of the University of Southern California, Los Angeles, California.

³ Emory Eye Center, Emory University School of Medicine, Atlanta, Georgia.

⁴ Department of Ophthalmology, Casey Eye Institute, Oregon Health and Science University, Portland, Oregon.

⁵ Ocular Oncology Service, Wills Eye Hospital, Thomas Jefferson University, Philadelphia, Pennsylvania.

⁶ Division of Ophthalmology, Department of Ophthalmology, Seattle Children's Hospital, University of Washington, Seattle, Washington.

⁷ Cancer and Blood Disease Institute, Children's Hospital Los Angeles, Los Angeles, California.

⁸ Norris Comprehensive Cancer Center, Keck School of Medicine, University of Southern California, Los Angeles, California.

⁹ The Saban Research Institute, Children's Hospital Los Angeles, Los Angeles, California.

Disclosures:

All authors have completed and submitted the ICMJE disclosures form.

The authors made the following disclosures: J.L.B. and L.X.: Patent application entitled: Aqueous humor cell free DNA for diagnostic and prognostic evaluation of ophthalmic disease.

J.L.B.: Research support – National Cancer Institute of the National Institute of Health Award Number K08CA232344, The Wright Foundation, Children's Oncology Group/ St. Baldrick's Foundation, Danhaki Family Foundation, Hyundai Hope on Wheels, Childhood Eye Cancer Trust, Children's Cancer Research Fund, A. Linn Murphree, MD, Chair in Ocular Oncology, The Berle & Lucy Adams Chair in Cancer Research, The Larry

and Celia Moh Foundation, The Institute for Families, Inc, Children's Hospital Los Angeles.

L.X.: Research support – The Knights Templar Eye Foundation.

A.N.: Research support – NIH K08EY030924, the Las Madrinan Endowment in Experimental Therapeutics for Ophthalmology, Research to Prevent Blindness Career Development Award, Knights Templar Eye Foundation Endowment.

H.E.G.: Research support – NIH R01 EY028450.

G.B.H.: Research support – the National Eye Institute as Protocol Co-Chair for studies on retinopathy of prematurity (ROP3 and ROP4 Trials).

The sponsors or funding organizations had no role in the design or conduct of this research.

Drs Alison Skalet and Kellyn Bellsmith are supported by grant P30 EY010572, from the National Institutes of Health (Bethesda, MD), and by unrestricted departmental funding from Research to Prevent Blindness (New York, NY).

HUMAN SUBJECTS: Human Subjects were used in this study. Institutional Review Board approval was obtained at Children's Hospital Los Angeles, University of Southern California (IRB CHLA-17-00248). The study was conducted in accordance with the Declaration of Helsinki. Written informed consent was obtained from the parents of all participants and that included permission for publication.

No animal subjects were used in this study.

Author Contributions:

Conception and design: Xu, Berry

Analysis and interpretation: Im, Pike, Reid, Peng, Xu, Berry

Data Collection: Im, Pike, Peng, Grossniklaus, Hubbard, Skalet, Bellsmith, Shields, Lally, Stacey, Reiser, Nagiel, Shah, Xu, Berry

Obtained funding: N/A

Overall responsibility: Im, Pike, Reid, Peng, Sirivolu, Grossniklaus, Hubbard, Skalet, Bellsmith, Shields, Lally, Stacey, Reiser, Nagiel, Shah, Xu, Berry

Abbreviations and Acronyms:

AH = aqueous humor; **BEV** = sample taken at bevacizumab injection; **cfDNA** = cell-free DNA; **dsDNA** = double-stranded DNA; **DX** = diagnostic sample; **END** = sample taken after completing retinoblastoma treatment; **IIRC** = International Intraocular Retinoblastoma Classification; **miRNA** = micro-RNA; **PRD** = pediatric retinal disease; **RB** = retinoblastoma; **RBI** = retinoblastoma 1 gene; **SCNA** = somatic copy number alteration; **SNV** = single-nucleotide variants; **ssDNA** = single-stranded DNA; **TX** = sample taken during retinoblastoma treatment.

Keywords:

Aqueous humor, Liquid biopsy, Circulating analytes, Retinoblastoma, Multicenter.

Correspondence:

Jesse L. Berry, MD, Director of Ocular Oncology, Children's Hospital Los Angeles, 4650 Sunset Blvd, Los Angeles, CA 90027. E-mail: Jesse.Berry@med.usc.edu.

References

- Karcioglu ZA, Gordon RA, Karcioglu GL. Tumor seeding in ocular fine needle aspiration biopsy. *Ophthalmology*. 1985;92:1763–1767.
- Berry JL, Xu L, Murphree AL, et al. Potential of aqueous humor as a surrogate tumor biopsy for retinoblastoma. *JAMA Ophthalmol*. 2017;135:1221–1230.
- Berry JL, Cobrinik D, Hicks J. Potential of aqueous humor as a surrogate tumor biopsy for retinoblastoma-reply. *JAMA Ophthalmol*. 2018;136:598.
- Berry JL, Xu L, Kooi I, et al. Genomic cfDNA analysis of aqueous humor in retinoblastoma predicts eye salvage: the surrogate tumor biopsy for retinoblastoma. *Mol Cancer Res*. 2018;16:1701–1712.
- Kim ME, Polski A, Xu L, et al. Comprehensive somatic copy number analysis using aqueous humor liquid biopsy for retinoblastoma. *Cancers (Basel)*. 2021;13:3340.
- Xu L, Shen L, Polski A, et al. Simultaneous identification of clinically relevant *RBI* mutations and copy number alterations in aqueous humor of retinoblastoma eyes. *Ophthalmic Genet*. 2020;41:526–532.
- Xu L, Polski A, Prabakar RK, et al. Chromosome 6p amplification in aqueous humor cell-free DNA is a prognostic biomarker for retinoblastoma ocular survival. *Mol Cancer Res*. 2020;18:1166–1175.
- Xu L, Kim ME, Polski A, et al. Establishing the clinical utility of ctDNA analysis for diagnosis, prognosis, and treatment monitoring of retinoblastoma: the aqueous humor liquid biopsy. *Cancers (Basel)*. 2021;13:1282.
- Polski A, Xu L, Prabakar RK, et al. Cell-free DNA tumor fraction in the aqueous humor is associated with therapeutic response in retinoblastoma patients. *Transl Vis Sci Technol*. 2020;9:30.
- Li HT, Xu L, Weisenberger DJ, et al. Characterizing DNA methylation signatures of retinoblastoma using aqueous humor liquid biopsy. *Nat Commun*. 2022;13:5523.
- Liu J, Ottaviani D, Sefta M, et al. A high-risk retinoblastoma subtype with stemness features, dedifferentiated cone states and neuronal/ganglion cell gene expression. *Nat Commun*. 2021;12:5578.
- Wong EY, Xu L, Shen L, et al. Inter-eye genomic heterogeneity in bilateral retinoblastoma via aqueous humor liquid biopsy. *NPJ Precis Oncol*. 2021;5:73.
- Berry JL, Xu L, Polski A, et al. Aqueous humor is superior to blood as a liquid biopsy for retinoblastoma. *Ophthalmology*. 2020;127:552–554.
- Ghose N, Kaliki S. Liquid biopsy in retinoblastoma: a review. *Semin Ophthalmol*. 2022;37:813–819.
- Gerrish A, Stone E, Clokie S, et al. Non-invasive diagnosis of retinoblastoma using cell-free DNA from aqueous humour [published correction appears in *Br J Ophthalmol*. 2020 Mar;104(3):415–416]. *Br J Ophthalmol*. 2019;103:721–724.
- Le Gall J, Dehainault C, Benoist C, et al. Highly sensitive detection method of retinoblastoma genetic predisposition and biomarkers. *J Mol Diagn*. 2021;23:1714–1721.
- Raval V, Racher H, Wrenn J, Singh AD. Aqueous humor as a surrogate biomarker for retinoblastoma tumor tissue. *J AAPOS*. 2022;26:137.e1–137.e5.
- Gerrish A, Jenkinson H, Cole T. The impact of cell-free DNA analysis on the management of retinoblastoma. *Cancers (Basel)*. 2021;13:1570.
- Liu W, Luo Y, Dai J, et al. Monitoring retinoblastoma by machine learning of aqueous humor metabolic fingerprinting. *Small Methods*. 2022;6:e2101220.
- Cancellieri F, Peter VG, Quinodoz M, et al. Genetic bases of retinoblastoma from liquid biopsies. *Invest Ophthalmol Vis Sci*. 2022;63:503. A0080.
- Alfaar AS, Chantada G, Qaddoumi I. Survivin is high in retinoblastoma, but what lies beneath? *J AAPOS*. 2018;22:482.
- Busch MA, Haase A, Miroshnikov N, et al. TFF1 in aqueous humor—a potential new biomarker for retinoblastoma. *Cancers (Basel)*. 2022;14:677.
- Ghiam BK, Xu L, Berry JL. Aqueous humor markers in retinoblastoma, a review. *Transl Vis Sci Technol*. 2019;8:13.
- Wierenga APA, Cao J, Mouthaan H, et al. Aqueous humor biomarkers identify three prognostic groups in uveal melanoma. *Invest Ophthalmol Vis Sci*. 2019;60:4740–4747.
- Kim ME, Xu L, Prabakar RK, et al. Aqueous humor as a liquid biopsy for retinoblastoma: clear corneal paracentesis and genomic analysis. *J Vis Exp*. 2021. <https://doi.org/10.3791/62939>.
- Baslan T, Kendall J, Rodgers L, et al. Genome-wide copy number analysis of single cells [published correction appears in *Nat Protoc*. 2016 Mar;11(3):616]. *Nat Protoc*. 2012;7:1024–1041.
- Sirivolu S, Xu L, Warren M, et al. Chromosome 6p amplification detected in blood cell-free DNA in advanced intraocular retinoblastoma. *Ophthalmic Genet*. 2022;43:866–870.
- Kooi IE, Mol BM, Massink MP, et al. A meta-analysis of retinoblastoma copy numbers refines the list of possible driver genes involved in tumor progression. *PLoS One*. 2016;11:e0153323.
- Polski A, Xu L, Prabakar R, et al. Longitudinal aqueous humor sampling reflects treatment response in retinoblastoma patients. *Invest Ophthalmol Vis Sci*. 2020;61:1394.
- Stathopoulos C, Gaillard MC, Moulin A, et al. Intravitreal anti-vascular endothelial growth factor for the management of neovascularization in retinoblastoma after intravenous and/or intraarterial chemotherapy: long-term outcomes in a series of 35 eyes. *Retina*. 2019;39:2273–2282.